



BIOREMEDIATION SCIENCE & TECHNOLOGY RESEARCH

Website: <http://journal.hibiscuspublisher.com/index.php/BSTR/index>



Mathematical Modeling of Molybdenum-Blue Production from *Bacillus* sp. strain Neni-10

Rusnam¹, Hafeez Muhammad Yakasai^{2*}, Mohd Fadhil Rahman³, Neni Gusmanizar⁴ and Mohd Yunus Shukor³

¹Department of Agricultural Engineering, Faculty of Agricultural Technology,
Andalas University, Padang, 25163, Indonesia.

²Department of Department of Biochemistry, Faculty of Basic Medical Sciences, College of Health Science,
Bayero University Kano, P. M. B 3011, Nigeria.

³Department of Biochemistry, Faculty of Biotechnology and Biomolecular Sciences,
Universiti Putra Malaysia, UPM 43400 Serdang, Selangor, Malaysia.

⁴Department of Animal Nutrition, Faculty of Animal Science, Andalas University,
Padang, 25163, Indonesia.

*Corresponding author:

Dr Hafeez Muhammad Yakasai,
Department of Biochemistry,
Faculty of Basic Medical Sciences,
College of Health Science,
Bayero University,
Kano,
Nigeria

Email: hmyakasai.bch@buk.edu.ng

HISTORY

Received: 18th April 2021
Received in revised form: 24th June 2021
Accepted: 15th July 2021

KEYWORDS

nonlinear regression
mathematical modelling
simulation
bacteria
heavy metal

ABSTRACT

Heavy metals can be remediated using microorganism by altering the redox function i.e. reduction from more toxic oxidation state to non-toxic one. Molybdenum reduction to molybdenum blue by bacteria is an emerging tool for remediation of the metal. Mathematical modelling via nonlinear regression of the heavy metal's reduction can yield important reduction parameters such as theoretical maximum reduction, specific reduction rate, and the lag period of reduction. Nonlinear regression can be utilized using various models such as logistic, Richards, Gompertz, Baranyi-Roberts, Schnute, Buchanan 3-phase, Von Bertalanffy and Huang with the best model yielding an underlying mechanistic property for the reduction. We demonstrate that the Baranyi-Roberts model was the best model in modelling the Mo-blue production curve of the bacterium *Bacillus* sp. strain Neni-10 based on statistical tests such as root-mean-square error (RMSE), corrected AICc (Akaike Information Criterion), adjusted coefficient of determination (R^2), accuracy factor (AF) and bias factor (BF). The model parameters or constants obtained were maximum lag time (λ), Mo-blue production rate (μ_m), and maximal Mo-blue production (Y_{max}). The construction of secondary models will benefit greatly from the use of bacterial growth models to acquire realistic Mo-blue production rates. According to a literature search, this technique is wholly unique for molybdenum reduction to Mo-blue in particular, and in the heavy metals' detoxification process in general. The results of this study have demonstrated the usefulness of these models in simulating Mo-blue synthesis in bacteria.

INTRODUCTION

Bacterial growth-linked processes frequently display a unique phase in which the specific growth rate of the bacterium begins at zero and then quickly accelerates reaching a maximal point. It has been resolved that those processes involved a specific growth rate with a value of zero, after which it begins to increase (μ_{max}) in a certain time period, producing a lag time (λ). It has been argued that the lag period seen in the sigmoid shape is because

the bacterial cells are gearing their growth mechanism to adjust to a new environment having been in a vegetative state especially during storage. This period is customarily called the lag period. It has been suggested as a transient period that connects two autonomous systems. The introduction of the lag time or parameter is meant largely convenience rather than having a mechanistic interpretation [1]. It is theorized that in the initial inocula, each bacterial cells would have different rates of

growth and if these rates are to be measured, would have shown a nonlinear distribution as suggested by researchers [1,2].

An emerging metal pollution: molybdenum has numerous applications, including in the manufacture of steel, corrosion-resistant steel component, engine anti-freeze additive and molybdenum disulfide in lubricant. Several cases of soil and water pollution have occurred due to the use of molybdenum in industry [3]. Molybdenum is highly toxic with cows with most affected to ruminants at a level as low as several parts per million and is due to the hypercuprosis phenomenon [4,5]. Mo-reducing bacteria are central to the bioremediation of this metal and to date, several are locally isolated [6–13] with the exception of a few [14–18]. Not many works on reducing molybdenum as a detoxification process due to the metal’s perceived low toxicity in humans in comparison to other heavy metals, such as mercury, selenium and chromium. However, the latest data shows that molybdenum is toxic in animal models and has play a role in sperm inhibition and embryogenesis arrest in organisms like catfish and mouse [19,20].

Several kinetic studies on Mo-blue production have been explored previously [21,22] but all of these works utilize the linearization of the Mo-blue production over time profile to obtain the specific growth rate for further secondary modelling. As the benefits of nonlinear regression analysis of the Mo-blue production have been described above, thus, the objective of this work is to evaluate several available models such as Logistic (Ricker, 1979; Zwietering *et al.* 1990), Gompertz [24,25], Richards [24,26], Schnute [24], Baranyi-Roberts [27], Von Bertalanffy [28,29], Buchanan three-phase [30] and more recently Huang model [31] (Table 1) in modeling Mo-blue production from the bacterium *Bacillus* sp. strain Neni-10.

MATERIALS AND METHODS

Isolation and maintenance of the molybdate-reducing bacterium

The bacterium was previously isolated, identified and characterized by Mansur *et al.* [11]. The growth and maintenance were carried out on solid agar in low phosphate medium (pH 7.0) [32] containing (NH₄)₂SO₄ (0.3%), Na₂MoO₄·2H₂O (0.242%), glucose (1%), NaCl (0.5%), MgSO₄·7H₂O (0.05%), yeast extract (0.05%), and Na₂HPO₄ (0.071% or 5 mM). Glucose was separately autoclaved.

Bacterial resting cells preparation

The study of the optimal conditions for reducing molybdenum from these bacteria in a microplate used resting or whole cells (microtiter) format [33]. To prepare resting cells without the presence of blue product, the LPM medium above was modified by excluding sodium molybdate and increasing the phosphate concentration to 100 mM. Overnight growth from a single colony inoculation into several 250 mL flasks with a total volume of 1 L was carried out at 120 rpm on an orbital shaker (Yihder, Taiwan). Cultures were pooled and cells were centrifuged at 15,000 × g for 10 min at room temperature. Pelleted cells with an approximate wet weight of 10 g were rinsed twice with sterile deionized water and resuspended in 20 mL of LPM with glucose omitted. Cell suspension of exactly 180 µL was transferred into the wells of a sterile microplate. Then 20 µL of sterile glucose or other carbon sources were added from a stock solution to the final concentration of 1.0 % (w/v). The final volume was 200 µL.

Table 1. Mo-blue production models used in this study.

No Model	No of parameters	Equation
1 Modified Logistic	3	$y = \frac{A}{\left\{ 1 + \exp \left[\frac{4\mu_m}{A} (\lambda - t) + 2 \right] \right\}}$
2 Modified Gompertz	3	$y = A \exp \left\{ - \exp \left[\frac{\mu_m e}{A} (\lambda - t) + 1 \right] \right\}$
3 Modified Richards	4	$y = A \left\{ 1 + \exp(1 + v) \exp \left[\frac{\mu_m}{A} (1 + v) \left(1 + \frac{1}{v} \right) (\lambda - t) \right] \right\}^{\left(\frac{-1}{v} \right)}$
4 Modified Schnute	4	$y = \left(\mu_m \frac{(1 - \beta)}{\alpha} \right) \left[\frac{1 - \beta \exp(\alpha \lambda + 1 - \beta - \alpha t)}{1 - \beta} \right]^{\frac{1}{\beta}}$
5 Baranyi-Roberts	4	$y = A + \mu_m x + \frac{1}{\mu_m} \ln \left(e^{-\mu_m x} + e^{-h_0} - e^{-\mu_m x - h_0} \right) - \ln \left(1 + \frac{e^{\mu_m x + \frac{1}{\mu_m} \ln \left(e^{-\mu_m x} + e^{-h_0} - e^{-\mu_m x - h_0} \right)} - 1}{e^{(y_{max} - A)}} \right)$
6 Von Bertalanffy	3	$y = K \left[1 - \left[1 - \left(\frac{A}{K} \right)^3 \right] \exp \left\{ \left(\mu_m x / 3K \right)^{\frac{1}{3}} \right\} \right]^3$
7 Huang	4	$y = A + y_{max} - \ln \left(e^A + \left(e^{y_{max} - A} \right) e^{-\mu_m B(x)} \right)$ $B(x) = x + \frac{1}{\alpha} \ln \frac{1 + e^{-\alpha(x-\lambda)}}{1 + e^{\alpha \lambda}}$
8 Buchanan Three-phase linear model	3	$y = A, \text{ if } x < \text{lag}$ $y = A + k(x - \lambda), \text{ if } \lambda \leq x \leq x_{max}$ $y = y_{max}, \text{ if } x \geq x_{max}$

Note:
 A= lower asymptote for Mo-blue;
 μ_m= maximum specific Mo-blue production rate;
 v= affects near which asymptote maximum for Mo-blue production occurs.
 λ=lag time
 y_{max}= Mo-blue upper asymptote;
 e = exponent (2.718281828)
 t = sampling time
 α, β, k = curve fitting parameters
 h₀ = a dimensionless parameter quantifying the initial physiological state of the reduction process.
 The lag time (h⁻¹) can be calculated as h₀=μ_{max}.

Addition of the carbon sources started Mo-blue production. Growth was measured at 600 nm while Mo-blue reduction was monitored at 750 nm (BioRad 680 (Richmond, CA, USA). To quantify Mo-blue production, the specific extinction coefficient of 11.69 mM⁻¹.cm⁻¹ at 750 nm was utilized. The readings at 750 nm must first be subtracted from readings at 600 nm to measure Mo-blue. This wavelength is the maximum filter available for the microplate unit [33].

Determination of Kinetic Parameters for Molybdenum Blue production

Fitting of the data

Nonlinear regression using the Marquardt algorithm (CurveExpert Professional software, Version 1.6) was used to align growth data with nonlinear equations. The sum of the squares of differences between the values predicted and observed was minimised in this lookup approach.

Statistical analysis

Multiple approaches were used to test if models had different parameters and whether the fit to the same experimental data was significant. Error functions utilized in this study include corrected AICc (Akaike Information Criterion), Root-Mean-Square Error (RMSE), bias factor (BF), accuracy factor (AF), and adjusted coefficient of determination (R^2). The model with fewer parameters is expected to yield lower RMSEs. The RMSE was calculated according to Eq. (1), where Ob_i , Pd_i , n and p are experimental data, predicted values, number of experimental data and number of parameters, respectively [34].

$$RMSE = \sqrt{\frac{\sum_{i=1}^n (Pd_i - Ob_i)^2}{n - p}} \quad \text{(Equation 1)}$$

The determination coefficient or R^2 will be used to evaluate the fitness quality of a model in linear regression. As the number of parameters can vary amongst the models used, a penalty function is introduced in a better version, which is the adjusted R^2 (equations 2 and 3) where s_y^2 is the total variance of the y -variable and RMS is Residual Mean Square.

$$Adjusted (R^2) = 1 - \frac{RMS}{s_y^2} \quad \text{(Equation 2)}$$

$$Adjusted (R^2) = 1 - \frac{(1 - R^2)(n - 1)}{(n - p - 1)} \quad \text{(Equation 3)}$$

The Akaike Information Criterion (AIC) is informational theory based and provides a model selection solution for the calculation of the relative quality of a particular statistical model for almost every single set of experimental data [35]. Data having a smaller number of values or a high number of parameter used are corrected with another version of AIC, which is the Akaike information criterion (AIC) with correction or AICc [36] and calculated according to the following equation (Eqn. 4);

$$AICc = 2p + n \ln \left(\frac{RSS}{n} \right) + 2(p+1) + \frac{2(p+1)(p+2)}{n-p-2} \quad \text{(Equation 4)}$$

Where n and p represent the number of data points in the curve and the number of parameters used in the model, respectively. For each data set, the model having the smallest AICc value is more likely correct [36]. Accuracy Factor (AF) and Bias Factor (BF) were calculated according to Eqns. 5 and 6 as suggested and first proposed by Ross [37]. A Bias Factor that is equal to 1 signifies an ideal match between observed and predicted values. For microbial growth curves or Mo-blue production studies, a bias factor having values < 1 signifies a fail-dangerous model whilst a bias factor having values > 1 signifies a model that is fail-safe.

The value of the Accuracy Factor is usually ≥ 1 , with higher AF values signifies prediction that is less precise or accurate.

$$\text{Bias factor} = 10^{\left(\frac{\sum_{i=1}^n \log \left(\frac{Pd_i / Ob_i}{n} \right)}{n} \right)} \quad \text{(Equation 5)}$$

$$\text{Accuracy factor} = 10^{\left(\frac{\sum_{i=1}^n \log \left(\frac{|Pd_i / Ob_i|}{n} \right)}{n} \right)} \quad \text{(Equation 6)}$$

RESULTS AND DISCUSSION

A sigmoidal shape profile of Mo-blue production from this bacterium was observed over time. A lag phase of about between 10 and 15 hours was observed. Maximum Mo-blue production occurred at approximately 50 hours after static incubation (Fig. 1). The sigmoidal shape is a typical growth process associated event seen in numerous Mo-reducing bacteria as the reduction of this metal is a growth associated process requiring reducing equivalents such as NADH that is often abundance during the exponential growth phase of bacterial growth [18]. During this lag phase, the bacteria are making adjustments to their surroundings. The population increases in a logarithmic manner once the lag phase is completed. Bacteria absorb nutrients as the population increases, producing waste products in the process.

When nutrition levels are low, the bacteria development rate slows down, which leads to an increase in the number of viable bacterium cells. The bacterial cell growth and cell death are both equal during the stationary phase. When the mortality rate is higher than the birth rate, the population enters the decline phase but this phase was not studied here [18]. Eight different growth models were utilized to fit the Mo-blue production over time. Model with the lowest value for RMSE, AICc and the highest value for adjusted R^2 is the best model. All of the fitting were visually acceptable (Fig. 2). Based on statistical analyses (Table 2), the best performance was the Baranyi-Roberts with good results for the error functions discriminant. The coefficients for the Baranyi-Roberts model at various molybdenum concentrations are shown in Table 3.

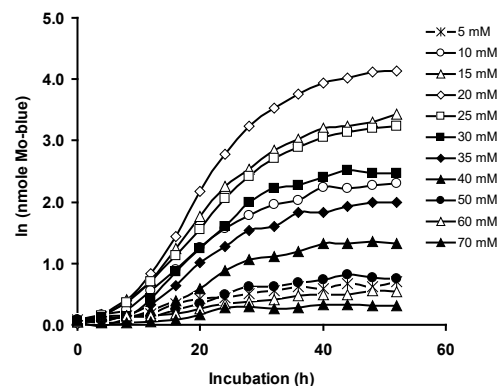


Fig. 1. The Mo-blue production curves of *Bacillus* sp. strain Neni-10 at various concentrations of sodium molybdate over time.

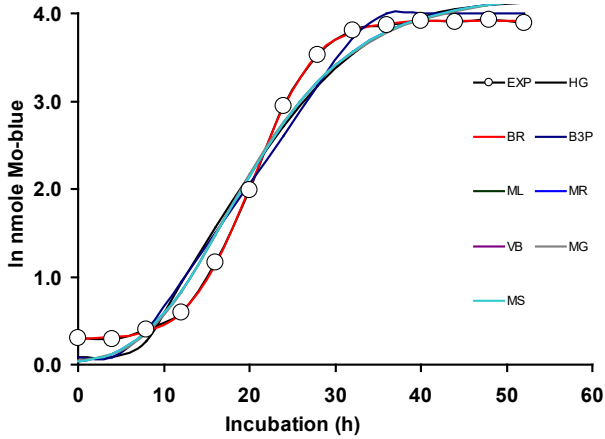


Fig. 2. The Mo-blue production curve of *Bacillus* sp. strain Neni-10 at 20 mM of sodium molybdate fitted to various models such as Huang (HG), Baranyi-Roberts (BR), Buchanan-three phase (B3P), modified Logistics (ML), modified Richards (MR), von Bertalanffy (VB), modified Gompertz (MG) and modified Schnute (MS).

Table 2. Statistical analysis of the various fitted models.

Model	p	RMSE	R ²	adR ²	AICc	BF	AF
Huang	4	0.048	0.999	0.999	-64.15	1.11	1.24
Baranyi-Roberts	4	0.128	0.994	0.991	-36.66	1.20	1.27
Buchanan-3-phase	3	0.020	0.994	0.993	-94.76	1.01	1.09
modified Logistics	3	0.089	0.997	0.996	-52.55	0.99	1.20
modified Richards	4	0.022	0.992	0.990	-86.42	0.82	1.24
von Bertalanffy	3	0.101	0.996	0.994	-49.04	0.58	1.88
modified Gompertz	3	0.022	0.997	0.999	-99.79	1.01	1.01
modified Schnute	4	0.089	0.997	0.995	-47.00	1.24	1.26

Note:
 p no of parameters
 RMSE Root mean square error
 adR² Adjusted Coefficient of determination
 BF Bias factor
 AF Accuracy factor

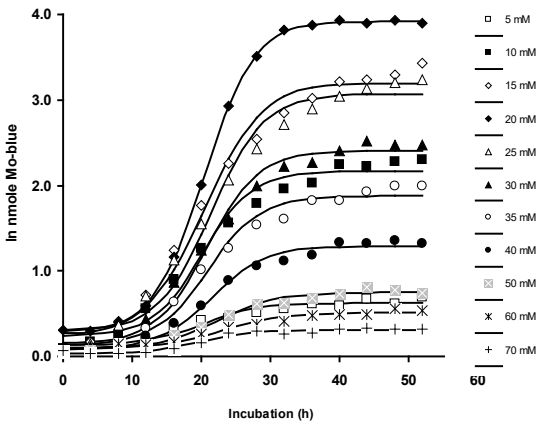


Fig. 3. The Mo-blue production curves of *Bacillus* sp. strain Neni-10 on various concentrations of sodium molybdate fitted to the Baranyi-Roberts model.

Table 3. Mo-blue production coefficients at various molybdenum concentrations as modelled using the Baranyi-Roberts model.

Asymptote (ln nmole Mo-blue)	Molybdenum concentration (mM)										
	5	10	15	20	25	30	35	40	50	60	70
Mo-blue	0.45	1.29	1.80	2.59	3.54	3.69	3.14	1.71	1.47	0.86	0.50
μ_m (h ⁻¹)	0.02	0.06	0.10	0.12	0.14	0.15	0.14	0.13	0.08	0.06	0.04
lag (h)	6.92	11.37	12.36	12.13	12.07	12.45	12.89	13.86	13.56	13.44	15.07

The Baranyi-Roberts model first proposed that a first-order differential equation (Equation 7) describes the variation of the cell population (x) with time [38];

$$\frac{dx}{dt} = \alpha(t)\mu(x)x \tag{Equation 7}$$

The following relationship for the production or growth rate is assumed (Equation 8)

$$\mu = \mu_{max} \left(1 - \frac{x}{x_{max}} \right) \tag{Equation 8}$$

The generic form of the model can be rewritten as

$$\mu(t) = \frac{1}{x(t)} \frac{dx}{dt} = \mu_{max} \alpha(t) f(t) \tag{Equation 9}$$

The $\alpha(t)$ function in the model assumes the presence of a bottle neck during growth which inhibits the lag phase and represented by $P(t)$. The manner of inhibition is similar to the Michaelis-Menten kinetics. The quotient q_0 represents the physiological state of the culture. The ratio between the substance $P(t)$ and its Michaelis-Menten constant is assumed to grow exponentially, from an initial value q_0 , at a constant vs specific rate. The $\alpha(t)$ increases monotonously with the limits $0 \leq \alpha \leq 1$ and $\lim_{t \rightarrow \infty} \alpha(t) = 1$ as follows (Equation 10);

$$\alpha(t) = \frac{P(t)}{P(t) + K_p} = \frac{q(t)}{1 + q(t)} = \frac{q_0}{q_0 + e^{-\mu_{max}t}} \tag{Equation 10}$$

The end-of-growth or end-of product formation inhibition is represented by the $f(t)$ function (Equation 11). It decreases monotonically with $f(0) = 1$ and $\lim_{t \rightarrow \infty} f(t) = 0$. The $f(t)$ function is described by a logistic inhibition function in most dynamics models as follows;

$$f(t) = 1 - \left(\frac{x}{x_{max}} \right) \tag{Equation 11}$$

Solutions to this differential equation was successfully worked out under certain fixed conditions, e.g. fixed temperatures (isothermal conditions). The penalty of the solution is for it having six parameters [1];

$$y = A + \mu_{max}x + \frac{1}{\mu_{max}} \ln \left(\frac{e^{-vt} + e^{-h_0} - e^{-vt-h_0}}{e^{m(\mu_{max}-A)}} \right) - \frac{1}{m} \ln \left(1 + \frac{e^{\frac{m\mu_{max}x + \frac{1}{\mu_{max}} \ln(e^{-vt} + e^{-h_0} - e^{-vt-h_0}) - 1}}}{e^{m(\mu_{max}-A)}} \right) \tag{Equation 12}$$

Where;

A represents the initial cell concentration (or product concentration), y_{max} is the asymptomatic cell concentration (or product concentration) in ln (CFU/ml) or ln product concentration, the curvature parameter is m , and this characterizes the shift from the exponential phase. A dimensionless parameter h_0 represents the initial physiological state of the cells, and v represents the curvature parameter to characterize the shift to the exponential phase. The lag time $\lambda(h)$ equals h_0/μ_{max} . The maximum specific growth rate ($1/h$) is represented as μ_{max} or μ_m .

The curvature parameters are suggested as follows; $v = \mu_{max}$ or μ_m and $m=1$ decreases the number of parameters by two causing the model to have only four parameters, which are μ_{max} ; h_0 ; A and y_{max} (Equation 12). It is proposed that h_0 may be considered as a fitness gauge of the micro-organism population towards the actual environment [1]. This fitness indicator can be more or less consistent when the experimental method is standardised and can be the same as assuming the lag time λ and the maximum specific growth rate μ_{max} is inversely proportional.

$$y = A + \frac{\mu_{max} x}{\mu_{max}} \ln \left(\frac{e^{-\mu_{max} x} + e^{-h_0} - e^{-\mu_{max} x - h_0}}{e^{(y_{max}-A)}} - 1 \right) \quad \text{(Equation 13)}$$

Compared to the modified Gompertz model, the Baranyi-Roberts model has been hinted to mostly be a lot more mechanistic in qualities meaning its parameters might be accorded biological meaning. This is despite the model having 4 parameters to be fitted. One suggested approach to raise the statistical significant of a mechanistic model with four parameter over a non-mechanistic three-parameter model is usually to increase the number of sets of data obtained [24]. Previous studies on models fitting Mo-blue production shows that the modified Gompertz model is the best model in several Mo-reducing bacteria (Table 4) and only one study reported von Bertalanffy as the best model.

Table 4. Mo-blue production models used in some previous studies.

Model	p	Best model for Mo-reducing bacterium	Ref
Modified Logistic	3	nil	
Modified Gompertz	3	<i>Bacillus amyloliquefaciens</i> strain Neni-9 <i>Bacillus</i> sp. strain Neni-12 <i>Serratia</i> sp. strain HMY1 <i>Burkholderia</i> sp. strain neni-11 <i>Bacillus</i> sp. strain Zeid 14	[39–43]
Modified Richards	4	nil	
Modified Schnute	4	nil	
Baranyi-Roberts	4	This study	
Von Bertalanffy	3	nil	
Huang	4	<i>Serratia</i> sp. strain DrY5	[44]
Buchanan Three-phase model	3 linear	nil	

The Baranyi and Roberts model has been used successfully to simulate microbial growth curves, such as *Bacillus* spp., *Brochothrix thermosphacta*, *Escherichia coli* O157:H7, *Listeria monocytogenes*, *Staphylococcus* spp., *Clostridium* spp., *Salmonella* Typhimurium and *Yersinia enterocolitica* [1,27,29,45,46]. In addition, the Baranyi-Roberts model has found application in modelling algae growth [47,48]. The model is preferred because of a number of factors: firstly, exhibits an excellent fitting capability; secondly, the model is appropriate under dynamic environmental situations, and thirdly, the majority of the model parameters do have biological meaning [29,49]. The parameters maximum lag time (λ), Mo-blue production rate (μ_m) and maximal Mo-blue production (Y_{max}) were the outputs of the modelling exercise. The biological parameters generated at this stage will be utilised later for

secondary modelling, such as using the Monod two-parameter model or other more advanced models such as Haldane, Aiba, Yano and others. The physical, chemical and biological mechanisms that contribute to the growth profile are all mechanistic models, which are mostly employed in fundamental research. Meaningful patterns can be more accurately predicted using a mechanistic model. Extrapolation beyond the reported circumstances makes them more likely to operate correctly [50].

CONCLUSION

Based on error function analysis, it can be concluded that the best model for fitting molybdenum-blue production in *Bacillus* sp. strain Neni-10 was Baranyi-Roberts. The fitting exercise gave important parameters such as maximum Mo-blue production rate (μ_m), lag time (λ) and maximal Mo-blue production, respectively. This is a unique method for obtaining accurate Mo-blue production rate that will be beneficial in developing further secondary models. This study shows that bacterial growth models are applicable to this procedure in the field of heavy metals detoxification, particularly Mo-blue production. Works underway include further secondary modelling for the values of Mo-blue production rate of the bacteria that we studied, particularly with regard to the impact of a growth substrate (molybdenum) on reduction. Other studies aimed at clarifying the molecular mechanisms underlying Mo-blue formation include the analysis of environmental factors such as pH and temperature.

REFERENCES

- Baranyi J, Roberts TA. A dynamic approach to predicting bacterial growth in food. *Int J Food Microbiol.* 1994;23(3–4):277–94.
- Buchanan RL, Whiting RC, Damert WC. When is simple good enough: A comparison of the Gompertz, Baranyi, and three-phase linear models for fitting bacterial growth curves. *Food Microbiol.* 1997;14(4):313–26.
- Neunhäuserer C, Berreck M, Insam H. Remediation of soils contaminated with molybdenum using soil amendments and phytoremediation. *Water Air Soil Pollut.* 2001;128(1–2):85–96.
- Underwood EJ. Environmental sources of heavy metals and their toxicity to man and animals. 1979;11(4–5):33–45.
- Kincaid RL. Toxicity of ammonium molybdate added to drinking water of calves. *J Dairy Sci.* 1980;63(4):608–10.
- Shukor MY, Habib SHM, Rahman MFA, Jirangon H, Abdullah MPA, Shamaan NA, et al. Hexavalent molybdenum reduction to molybdenum blue by *S. marcescens* strain Dr. Y6. *Appl Biochem Biotechnol.* 2008;149(1):33–43.
- Rahman MFA, Shukor MY, Suhaili Z, Mustafa S, Shamaan NA, Syed MA. Reduction of Mo(VI) by the bacterium *Serratia* sp. strain DR Y5. *J Environ Biol.* 2009;30(1):65–72.
- Lim HK, Syed MA, Shukor MY. Reduction of molybdate to molybdenum blue by *Klebsiella* sp. strain hkeem. *J Basic Microbiol.* 2012;52(3):296–305.
- Abo-Shakeer LKA, Ahmad SA, Shukor MY, Shamaan NA, Syed MA. Isolation and characterization of a molybdenum-reducing *Bacillus pumilus* strain lbna. *J Environ Microbiol Toxicol.* 2013;1(1):9–14.
- Othman AR, Bakar NA, Halimi MIE, Johari WLW, Ahmad SA, Jirangon H, et al. Kinetics of molybdenum reduction to molybdenum blue by *Bacillus* sp. strain A.rzi. *BioMed Res Int.* 2013;2013:Article number 371058.
- Mansur R, Gusmanizar N, Roslan MAH, Ahmad SA, Shukor MY. Isolation and characterisation of a molybdenum-reducing and Metanil yellow dye-decolourising *Bacillus* sp. strain Neni-10 in soils from West Sumatera, Indonesia. *Trop Life Sci Res.* 2017 Jan;28(1):69–90.
- Kesavan V, Mansur A, Suhaili Z, Salihan MSR, Rahman MFA, Shukor MY. Isolation and Characterization of a Heavy Metal-reducing *Pseudomonas* sp. strain Dr.Y Kertih with the Ability to

- Assimilate Phenol and Diesel. *Bioremediation Sci Technol Res.* 2018 Jul 31;6(1):14–22.
13. Maarof MZ, Shukor MY, Mohamad O, Karamba KI, Halmi MIE, Rahman MFA, et al. Isolation and Characterization of a Molybdenum-reducing *Bacillus amyloliquefaciens* strain KIK-12 in Soils from Nigeria with the Ability to grow on SDS. *J Environ Microbiol Toxicol.* 2018 Jul 31;6(1):13–20.
 14. Capaldi A, Proskauer B. Beiträge zur Kenntniss der Säurebildung bei Typhus-bacillen und Bacterium coli - Eine differential-diagnostische Studie. *Z Für Hyg Infect.* 1896;23(3):452–74.
 15. Levine VE. The reducing properties of microorganisms with special reference to selenium compounds. *J Bacteriol.* 1925;10(3):217–63.
 16. Campbell AM, Del Campillo-Campbell A, Villaret DB. Molybdate reduction by *Escherichia coli* K-12 and its chl mutants. *Proc Natl Acad Sci U S A.* 1985;82(1):227–31.
 17. Khan A, Halmi MIE, Shukor MY. Isolation of Mo-reducing bacterium in soils from Pakistan. *J Environ Microbiol Toxicol.* 2014;2(1):38–41.
 18. Yakasai HM, Rahman MF, Manogaran M, Yasid NA, Syed MA, Shamaan NA, et al. Microbiological Reduction of Molybdenum to Molybdenum Blue as a Sustainable Remediation Tool for Molybdenum: A Comprehensive Review. *Int J Environ Res Public Health.* 2021 Jan;18(11):5731.
 19. Yamaguchi S, Miura C, Ito A, Agusa T, Iwata H, Tanabe S, et al. Effects of lead, molybdenum, rubidium, arsenic and organochlorines on spermatogenesis in fish: Monitoring at Mekong Delta area and in vitro experiment. *Aquat Toxicol.* 2007;83(1):43–51.
 20. Zhang Y-L, Liu F-J, Chen X-L, Zhang Z-Q, Shu R-Z, Yu X-L, et al. Dual effects of molybdenum on mouse oocyte quality and ovarian oxidative stress. *Syst Biol Reprod Med.* 2013;59(6):312–8.
 21. Halmi MIE, Ahmad SA, Syed MA, Shamaan NA, Shukor MY. Mathematical modelling of the molybdenum reduction kinetics in *Bacillus pumilus* strain Lbna. *Bull Environ Sci Manag.* 2014;2(1):24–9.
 22. Othman AR, Bakar NA, Halmi MIE, Johari WLW, Ahmad SA, Jirangon H, et al. Kinetics of molybdenum reduction to molybdenum blue by *Bacillus* sp. strain A.rzi. *BioMed Res Int.* 2013;2013.
 23. Ricker, F.J. 11 Growth Rates and Models. In: W.S. Hoar DJR and JRB, editor. *Fish Physiology* [Internet]. Academic Press; 1979 [cited 2014 Jun 27]. p. 677–743. (Bioenergetics and Growth; vol. Volume 8). Available from: <http://www.sciencedirect.com/science/article/pii/S1546509808600345>
 24. Zwietering MH, Jongenburger I, Rombouts FM, Van't Riet K. Modeling of the bacterial growth curve. *Appl Environ Microbiol.* 1990;56(6):1875–81.
 25. Gompertz B. On the nature of the function expressive of the law of human mortality, and on a new mode of determining the value of life contingencies. *Philos Trans R Soc London.* 1825;115:513–85.
 26. Richards, F.J. A flexible growth function for empirical use. *J Exp Bot.* 1959;10:290–300.
 27. Baranyi J. Mathematics of predictive food microbiology. *Int J Food Microbiol.* 1995;26(2):199–218.
 28. Babák L, Šupinová P, Burdychová R. Growth models of *Thermus aquaticus* and *Thermus scotoductus*. *Acta Univ Agric Silvicae Mendel Brun.* 2012;60(5):19–26.
 29. López S, Prieto M, Dijkstra J, Dhanoa MS, France J. Statistical evaluation of mathematical models for microbial growth. *Int J Food Microbiol.* 2004;96(3):289–300.
 30. Buchanan RL. Predictive food microbiology. *Trends Food Sci Technol.* 1993;4(1):6–11.
 31. Huang L. Optimization of a new mathematical model for bacterial growth. *Food Control.* 2013;32(1):283–8.
 32. Rahman MF, Rusnam M, Gusmanizar N, Masdor NA, Lee CH, Shukor MS, et al. Molybdate-reducing and SDS-degrading *Enterobacter* sp. Strain Neni-13. *Nova Biotechnol Chim.* 2016 Dec 1;15(2):166–81.
 33. Shukor MS, Shukor MY. A microplate format for characterizing the growth of molybdenum-reducing bacteria. *J Environ Microbiol Toxicol.* 2014;2(2):42–4.
 34. Motulsky HJ, Ransnas LA. Fitting curves to data using nonlinear regression: a practical and nonmathematical review. *FASEB J Off Publ Fed Am Soc Exp Biol.* 1987;1(5):365–74.
 35. Akaike H. New look at the statistical model identification. *IEEE Trans Autom Control.* 1974;AC-19(6):716–23.
 36. Burnham KP, Anderson DR. *Model Selection and Multimodel Inference: A Practical Information-Theoretic Approach.* Springer Science & Business Media; 2002. 528 p.
 37. Ross T, McMeekin TA. Predictive microbiology. *Int J Food Microbiol.* 1994;23(3–4):241–64.
 38. Perni S, Andrew PW, Sharma G. Estimating the maximum growth rate from microbial growth curves: definition is everything. *Food Microbiol.* 2005;491–495(6):491–5.
 39. Adnan M, Abu Zeid I, Ahmad SA, Effendi Halmi M, Abdullah S, Shukor M. A Molybdenum-reducing *Bacillus* sp. Strain Zeid 14 in Soils from Sudan that Could Grow on Amides and Acetonitrile. *Malays J Soil Sci.* 2016 Jan 1;20:111–34.
 40. Mansur R, Gusmanizar N, Dahalan FA, Masdor NA, Ahmad SA, Shukor MS, et al. Isolation and characterization of a molybdenum-reducing and amide-degrading *Burkholderia cepacia* strain neni-11 in soils from west Sumatera, Indonesia. *IIOAB.* 2016;7(1):28–40.
 41. Yakasai MH, Ibrahim KK, Yasid NA, Halmi MIE, Rahman MFA, Shukor MY. Mathematical modelling of molybdenum reduction to mo-blue by a cyanide-degrading bacterium. *Bioremediation Sci Technol Res.* 2016 Dec 31;4(2):1–5.
 42. Rusnam, Gusmanizar N. Isolation and Characterization of a Molybdenum-reducing and Coumaphos-degrading *Bacillus* sp. strain Neni-12 in soils from West Sumatera, Indonesia. *J Environ Microbiol Toxicol.* 2019 Dec 31;7(2):20–5.
 43. Rusnam, Gusmanizar N. Isolation and Characterization of a Molybdenum-reducing and Carbamate-degrading *Bacillus amyloliquefaciens* strain Neni-9 in soils from West Sumatera, Indonesia. *Bioremediation Sci Technol Res.* 2020 Jul 31;8(1):17–22.
 44. Syed MA, Shamaan NA, Shukor MY. Mathematical Modeling of the Molybdenum Blue Production from *Serratia* sp. strain DRY5. *J Environ Microbiol Toxicol.* 2020 Dec 31;8(2):12–7.
 45. Coleman ME, Tamplin ML, Phillips JG, Marmer BS. Influence of agitation, inoculum density, pH, and strain on the growth parameters of *Escherichia coli* O157:H7 - Relevance to risk assessment. *Int J Food Microbiol.* 2003;83(2):147–60.
 46. Fujikawa H. Development of a new logistic model for microbial growth in foods. *Biocontrol Sci.* 2010;15(3):75–80.
 47. Lacerda LMCF, Queiroz MI, Furlan LT, Lauro MJ, Modenesi K, Jacob-Lopes E, et al. Improving refinery wastewater for microalgal biomass production and CO₂ biofixation: Predictive modeling and simulation. *J Pet Sci Eng.* 2011;78(3–4):679–86.
 48. Tevatia R, Demirel Y, Blum P. Kinetic modeling of photoautotrophic growth and neutral lipid accumulation in terms of ammonium concentration in *Chlamydomonas reinhardtii*. *Bioresour Technol.* 2012;119:419–24.
 49. Van Impe JF, Poschet F, Geeraerd AH, Vereecken KM. Towards a novel class of predictive microbial growth models. *Int J Food Microbiol.* 2005;100(1–3):97–105.
 50. Bolker BM. *Ecological Models and Data in R.* Princeton, N.J: Princeton University Press; 2008. 408 p.